Chemical Engineering Journal 159 (2010) 11–16

Contents lists available at ScienceDirect

Chemical Engineering Journal

journal homepage: www.elsevier.com/locate/cej

A model to predict fugitive VOC emissions from liquid charged flange joints with graphite gaskets

Christian Bramsiepe*, Lukas Pansegrau, Gerhard Schembecker

Faculty of Biochemical and Chemical Engineering, Laboratory for Plant and Process Design, Technische Universität Dortmund, Emil-Figge Straße 70, 44227 Dortmund, Germany

ARTICLE INFO

Article history:
Received 26 August 2009
Received in revised form 1 February 2010
Accepted 6 February 2010

Keywords:
Flange joint
Fugitive emission
Volatile organic compounds
Graphite sheet gasket

ABSTRACT

A model to describe the fugitive emission of volatile organic compounds from flange joints is presented. By combination of laminar and capillary flow in a new concept of branching capillaries, this conception increases the prediction accuracy compared to the existing model of linear capillaries. Furthermore a correlation is deduced to describe the capillary diameter as a function of gasket stress using the compression curve of the gasket. A model is developed and experimentally validated, which predicts fugitive emissions from liquid charged flange joints as a function of medium properties, pipe pressure, gasket width and gasket stress. Finally the parameters influencing the emission rate of liquid charged flange joints are discussed and recommendations for fugitive emission reduction are presented.

1. Introduction

Saving the world climate and guaranteeing the quality of atmospheric air is a major concern in the field of climate protection. As a consequence the majority of the industrial nations has launched programs to reduce emissions of greenhouse gases. As a result of these efforts, amongst others, the emission of volatile organic compounds (VOCs) could significantly be reduced. Though major reductions have been achieved by reducing direct emissions released from sources like flares and waste air streams, the emissions from fugitive sources like pump, armature and flange sealings, could also be confined (in the case of flange joints to an average emission rate of approximately 10^{-3} mg m^{-1} s^{-1} [1]). These advances were reached by improvements in the quality of dimensioning assured by technical guidelines (in Germany, e.g. [2,3]). On the other hand guidelines, that can be used to train the assembly personnel [4–7], allow for the technical implementation of dimensioning requirements. It can be anticipated, that flange joints, which exceed the expected emission range dramatically, will widely be eliminated in the long run by applying these guidances and by continuous maintenance activities.

For further emission reductions the gasket materials have to be optimized. Therefore, analyzing transport phenomena in an emitting liquid is essential. These investigations have to be based on laboratory investigations to eliminate the random influence of vibrations, temperature swings and start-up or shutdown processes, that occur in operating plants.

Models describing the mass transport through rubber-asbestos and graphite gaskets are already available for gases. Based on the capillary models presented by Micheely [8] and Kämpkes [9], a model to predict fugitive emissions from graphite gaskets has been developed by Hummelt et al. [10,11]. Considering the gasket as a solid pervaded by parallel linear capillaries, mass transport is described as Knudsen diffusion. In this model total emission is split into two streams: surface leakage and cross section leakage. First of which is the emission through the contact area of flanges and gasket, whereas the latter is the emission through the sealing material itself. The dependence of the emission rate on gasket stress is described by assuming the sealing material to be a linear elastic body.

Choi et al. [12] has published a first model conception for the emission of liquids. As he could not observe any dependency of liquid emission rates on bulk pressure in field data, he brought up the idea, that capillary forces determine the emission from liquid-charged flange joints. However laboratory investigations presented by Bramsiepe and Schembecker [1] affirm a significant correlation between liquid emission rate and pipe pressure and demonstrate, that in field data, the basic transport phenomena are overlaid by the random effect of assembly and maintenance. Liquid emission could be described as laminar flow driven by a combination of capillary forces and bulk pressure.

* Corresponding author. Tel.: +49 0 231 755 3213; fax: +49 0 231 755 2341.
E-mail addresses: Christian.Bramsiepe@bci.tu-dortmund.de (C. Bramsiepe), Lukas.Pansegrau@bci.tu-dortmund.de (L. Pansegrau), Gerhard.Schembecker@bci.tu-dortmund.de (G. Schembecker).
URL: http://www.apt.bci.tu-dortmund.de (C. Bramsiepe).

1385-8947/$ – see front matter © 2010 Elsevier B.V. All rights reserved.
doi:10.1016/j.cej.2010.02.014

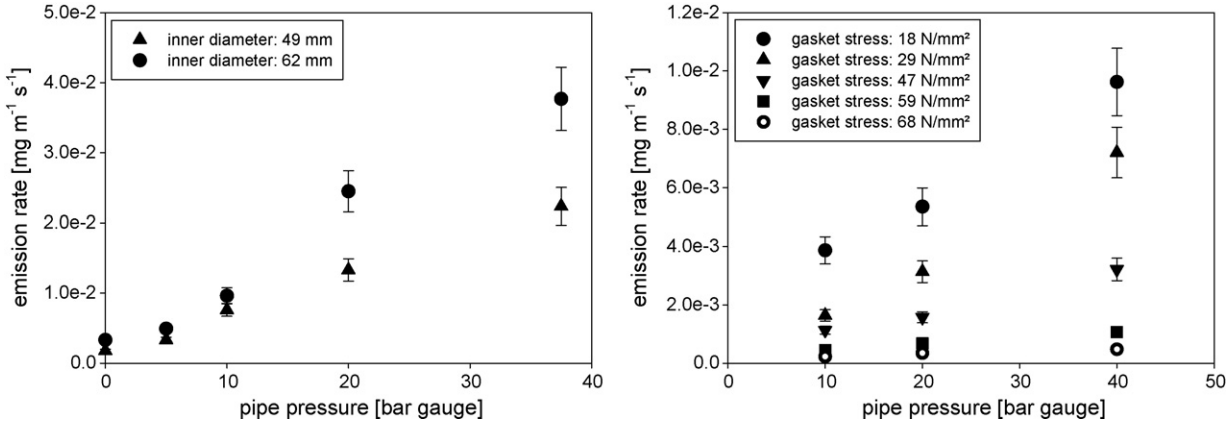

Fig. 1. *Left:* Emission rates of 1-propanol charged flange joints with Sigraflex® Universal Pro graphite sheet gaskets (outer diameter: 92 mm; height: 3 mm) at a gasket stress of 10 N/mm^2 in weld neck flanges with even raised faces nominal diameter *DN*40 and nominal pressure *PN*40 with a surface roughness of 6.2 μm as a function of pipe pressure and gasket width. *Right:* Emission rates of methanol charged flange joints with grooved gaskets (height of the graphite layer: 2 mm × 0.5 mm, inner diameter: 95 mm; outer diameter: 121 mm) in weld neck flanges with even raised faces nominal diameter *DN*80 and nominal pressure *PN*40 with a surface roughness of 40 μm as a function of pipe pressure and gasket stress.

2. Materials and methods

For the model validation, experimental results from methanol charged flange joints with grooved gaskets were used as published in [1].

Furthermore the emission rates were measured at 1-propanol charged flange joints with nominal diameter *DN*40 and nominal pressure *PN*40 with Sigraflex® Universal Pro graphite sheet gaskets from SGL Carbon Group with an outer diameter of 92 mm and an inner diameter of either 49 mm or 62 mm. The gaskets were 3 mm thick with two sheets of tanged steel. Six test points were installed in series and flanges with 6.2 μm surface roughness were used. The gasket stress was 10 N/mm^2.

The test procedure was identical for both types of gaskets and flanges and is described in [1]. The total organic carbon concentration was determined as propane equivalents with a flame ionization detector (FID) from Mess- und Analysetechnik GmbH Leverkusen operating at a sweeping gas flow rate of 25 l/h measured with a FMA1816 flow meter from Newport Electronics.

The gasket stress was applied with a calibrated torque wrench. Settling was monitored with feeler pin screws according to [13] and compensated after 24 h and again after 36 h by retightening the screws. All experiments were carried out at ambient temperature until steady state was observed (at least for 2 days).

3. Results and discussion

Fig. 1 (left) shows the emission rates of 1-propanol charged graphite sheet gaskets. These results were used to check the model describing the influence of pipe pressure on the emission rate. As it took several weeks to saturate the gaskets with the emitting liquid, methanol emission rates of grooved gaskets published in [1] were used to prove the model describing the influence of gasket stress on the emission rate (Fig. 1, right).

3.1. Model development

As graphite gaskets show a very complex sandwich structure instead of a capillary structure, modeling the gasket behavior required some simplifications. The following assumptions were made:

1. The gasket material has a constant porosity, depending only on the gasket stress.
2. The width of the gasket is independent from the gasket stress.
3. The number of capillaries is independent from the gasket stress (none of the capillaries is closed when the gasket is compressed).
4. The capillaries are not necessarily linear but they can branch.
5. All capillaries have the same diameter, which is constant with the radius.

3.1.1. Sealing structure

In the capillary models, mass transport takes place in linearly arranged parallel capillaries. This implies, that the velocity of the emitting component remains constant while passing the gasket.

As graphite sheet gaskets as well as the graphite layers of grooved gaskets are usually cut out of uniform plates, the porosity of the gasket material can be assumed to be constant all over the gasket. Especially for small-sized gaskets with a big ratio of outer to inner diameter – in this investigation this ratio was 1.48 for the narrow and 1.88 for the wide gasket – this precondition is not correct. Therefore the model was adapted by establishing a capillary network instead of parallel capillaries. Thus the number of capillaries per square meter gasket material remains constant (constant porosity) while the total number increases from the inner to the outer edge of the gasket material. Fig. 2 provides a graphical comparison of the previous (a) and the new concept (b).

The density of the capillaries (capillaries per m^2 gasket cross section area) N_{cap} [1/m^2] at the average gasket diameter was defined as

$$N_{cap} = \frac{n_{cap}}{\pi h_g \bar{d}_g} \quad (1)$$

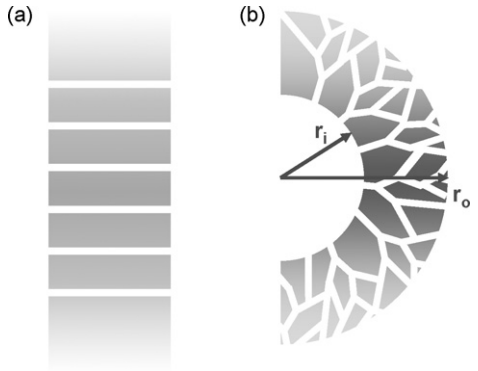

Fig. 2. Model of the gasket structure in the literature (a) and in this work (b).

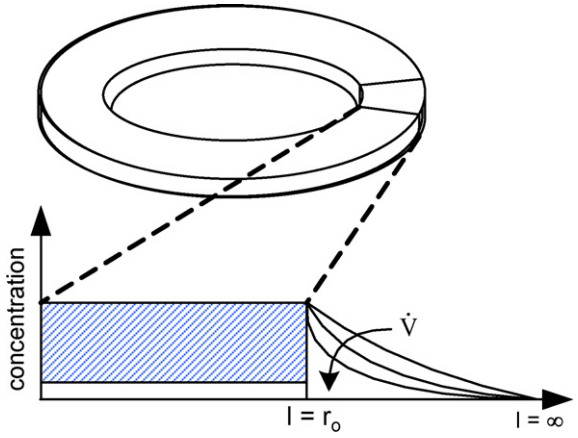

Fig. 3. Impact of the sweeping gas flow rate on the boundary layer thickness.

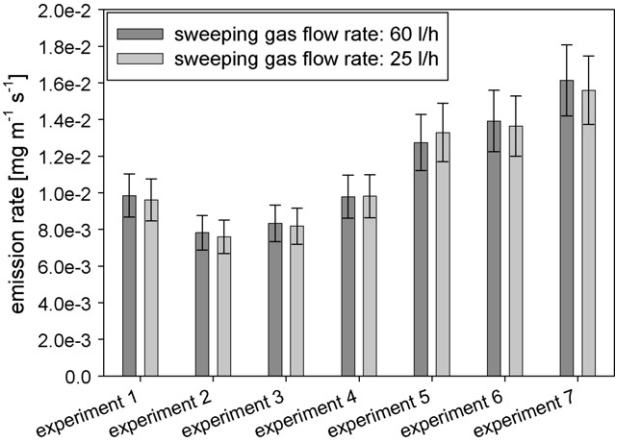

Fig. 4. Influence of the sweeping gas flow rate on the emission rate.

N_{cap} is independent from the radius of the gasket ($N_{cap} \neq f(r_g)$). Here $\bar{d}_g$ [m] is the average diameter of the gasket, n_{cap} is the number of capillaries at the average diameter and h_g [m] is the gasket height. According to the previous precondition 3 the number of capillaries is a function of gasket diameter but it is independent from the gasket stress.

3.1.2. Mass transport

In case of laminar or turbulent flow, the main driving force for mass transport of gases is the gradient of absolute pressure and in case of diffusion it is the gradient of partial pressure. As liquids have much higher surface tensions and viscosities than gases, for the mass transport of liquids additional effects must be taken into consideration.

At first the location has to be pinpointed, where the liquid–gas phase change takes place. To answer this question, a flange joint was charged with a sodium chloride solution in order to identify the point of phase change as the point, where the water evaporates and the dry salt remains. Unexpectedly no salt could be detected but corrosion was observed over the whole radius of the gasket. Therefore it can be assumed that the gasket is saturated with the emitting liquid and that the liquid–gas phase change takes place at the outer edge of the gasket.

Furthermore it had to be determined whether the overall mass transport is governed by the flow through the porous gasket or by the liquid gas phase change. If a boundary layer controls the mass flow at the outer edge of the gasket it will be influenced by the sweeping gas velocity. A variation of the sweeping gas flow rate would thus change the emission rate. The higher the flow rate, the thinner the boundary layer and the faster the mass transport. Fig. 3 displays this situation graphically.

To check this interrelation, a subset of measurements was executed with a sweeping gas flow rates of 25 l/h and 60 l/h.

As can be taken from Fig. 4, the flow rate of the sweeping gas did not have an impact on the emission rate. This is in accordance with the findings Altinkaya [17] presents for the evaporation of VOCs from coating materials. Therefore the impact of the phase change on the emission rate has been neglected in the model development.

The correlation between the emission rate of a linear capillary and the pipe pressure published in [1] was used to describe the mass transport within the gasket:

$$\dot{m}_E = -\frac{\rho}{\eta}\frac{\pi d_{cap}^4}{128}\frac{dp}{dr_g} \quad (2)$$

Here ρ [kg/m^3] is the density and η [kg s^{-1} m^{-1}] the dynamic viscosity of the emitting liquid, d_{cap} [m] is the diameter of the capillaries, p [Pa] the pressure of the emitting liquid within the gasket material and r_g [m] the radius of the gasket.

Furthermore the total driving force for the mass transport in liquid charged gaskets can be described as:

$$\Delta p_{total} = \Delta p_{bulk} + \Delta p_{cap} \quad (3)$$

In this equation Δp_{bulk} [Pa] is the difference between pipe pressure p_i [Pa] and ambient pressure p_a [Pa] and Δp_{cap} [Pa] is the capillary pressure. Fig. 5 illustrates the pressure characteristics within the gasket.

According to [14] the capillary pressure, which represents the pressure difference between ambient pressure and the pressure p_{inter} (Pa) in the interface between the emitting liquid and ambient

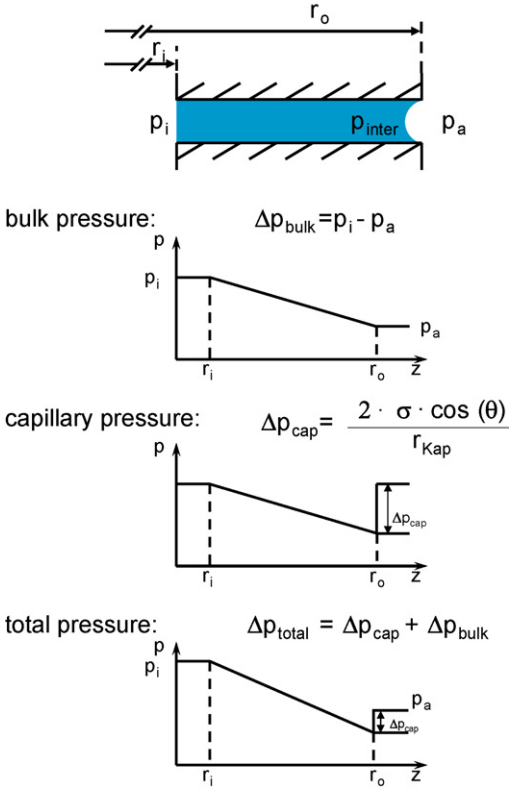

Fig. 5. Visualization of the pressure characteristics within a liquid charged gasket.

air, is given as

$$\Delta p_{cap} = p_a - p_{inter} = \frac{4\sigma\ \cos(\theta)}{d_{cap}} \tag{4}$$

σ [N/m] is the surface tension of the emitting liquid and θ [°] is the contact angle between the liquid and the gasket material.

Combining Eqs. (1) and (2), the emission rate is given as

$$\dot{m}_E = -N_{cap} h_g \pi^2 r_g \frac{\rho}{\eta} \frac{d_{cap}^4}{64} \frac{\partial p}{\partial r_g} \tag{5}$$

Integration leads to

$$\dot{m}_E \int_{r_i}^{r_o} \frac{1}{r_g} dr_g = -N_{cap} h_g \pi^2 r_g \frac{\rho}{\eta} \frac{d_{cap}^4}{64} \int_{p_i}^{p_{inter}} dp \tag{6}$$

$$\Rightarrow \quad \bar{\dot{m}}_E = N_{cap} h_g \frac{\rho}{\eta} \frac{d_{cap}^4 \pi^2}{64 \ln(r_o/r_i)(r_o + r_i)} (p_i - p_{inter}) \tag{7}$$

$\bar{\dot{m}}_E$ is the emission rate normalized to the average gasket diameter. With Eqs. (3) and (4) the emission rate is given as

$$\bar{\dot{m}}_E = N_{cap} h_g \frac{\rho}{\eta} \frac{\pi^2}{64 \ln(r_o/r_i)(r_o + r_i)} (d_{cap}^4 \Delta p_{bulk} + 4 d_{cap}^3 \sigma\ \cos(\theta)) \tag{8}$$

3.1.3. Gasket stress

In order to describe the porosity of the compressed gasket (ϵ) in dependency of the porosity of the unstressed gasket (ϵ_0) it can be assumed that all the compression takes place in the excavations, while the graphite itself is deformed but not compressed. Furthermore it can be assumed, that the weight of the dry gasket is only made up by graphite, whereas the weight of enclosed gas can be neglected.

$$\epsilon_g = \frac{V_{excav.}}{V_g} = 1 - \frac{V_{gr}}{V_g} = 1 - \frac{\rho_g}{\rho_{gr}} \tag{9}$$

ϵ_g is the porosity of the gasket, $V_{excav.}$ [m^3] is the volume of the excavations within the gasket, V_g [m^3] is the volume of the gasket, V_{gr} [m^3] is the volume of the graphite, ρ_g [kg/m^3] is the density of the whole gasket and ρ_{gr} [kg/m^3] is the density of the graphite. Assuming exclusively axial compression results in

$$\frac{V_g}{V_{g,0}} = \frac{h_g \pi (r_o^2 - r_i^2)}{h_{g,0} \pi (r_o^2 - r_i^2)} = \frac{h_g}{h_{g,0}} = \frac{\rho_{g,0}}{\rho_g} \tag{10}$$

With Eq. (9) this leads to

$$\epsilon_g = 1 - \frac{\rho_{g,0}}{\rho_{gr}} \frac{h_{g,0}}{h_g} \tag{11}$$

which is also valid for the unstressed gasket, which results in

$$\epsilon_g = 1 - (1 - \epsilon_{g,0}) \frac{h_{g,0}}{h_g} \tag{12}$$

The porosity of the gasket can be described as a function of capillary diameter and capillary density

$$\epsilon_g = N_{cap} \frac{\pi}{4} d_{cap}^2 \tag{13}$$

Using Eqs. (1) and (13) the dependency of the capillary diameter from gasket stress can be described using the correlation between gasket height and gasket stress.

$$\frac{\epsilon}{\epsilon_0} = \frac{h_0 d_{cap}^2}{h d_{cap,0}^2} \tag{14}$$

Thus the capillary diameter can be calculated as

$$d_{cap} = d_{cap,0} \sqrt{\frac{\epsilon h}{\epsilon_0 h_0}} = d_{cap,0} \sqrt{\frac{h - (1 - \epsilon_0) h_0}{\epsilon_0 h_0}} \tag{15}$$

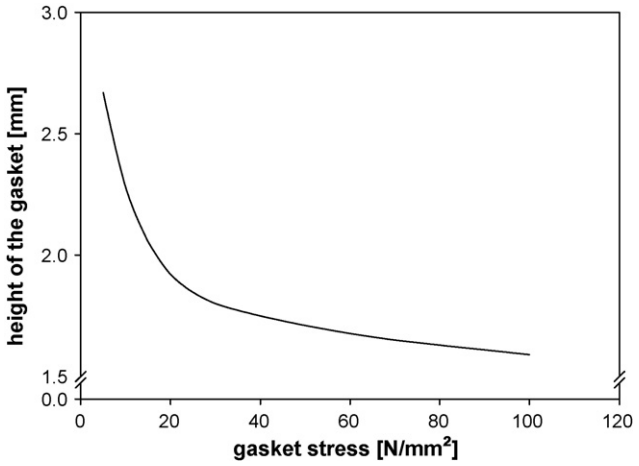

Fig. 6. Compression curve of a Sigraflex® Universal Pro gasket with two sheets of tanged steel and an uncompressed height of 3 mm [15].

With this equation and the height of the gasket as a function of gasket stress, which is typically available from the manufacturer (see Fig. 6), the capillary diameter can be calculated as a function of gasket stress.

Inserting Eq. (15) into Eq. (8), the emission rate can be described as a function of the geometry of the gasket, pipe pressure, medium properties and gasket stress (Eq. (16)).

$$\bar{\dot{m}}_E = N_{cap} h \frac{\rho}{\eta} \frac{\pi^2}{64 \ln(r_o/r_i)(r_o + r_i)^2} \left[\left(d_{cap,0} \sqrt{\frac{h - (1 - \epsilon_0) h_0}{\epsilon_0 h_0}} \right)^4 \Delta p_{bulk} \right] + N_{cap} h \frac{\rho}{\eta} \frac{\pi^2}{64 \ln(r_o/r_i)(r_o + r_i)^2} \left[4 \left(d_{cap,0} \sqrt{\frac{h - (1 - \epsilon_0) h_0}{\epsilon_0 h_0}} \right)^3 \sigma \cos(\theta) \right] \tag{16}$$

Though the derivation of the model equations in this paper is limited to graphite gaskets, the basic ideas could also be applied to other materials. In this case also the aging of the gasket could be regarded by making capillary diameter and capillary density dependent on time. Graphite gaskets usually are expected not to age.

3.2. Model validation

To validate the approach of branching capillaries the emission rates of gaskets with 49 mm inner diameter and the emission rates of those with 62 mm inner diameter were compared. Both types of gaskets had 92 mm outer diameter. Using the model of linear capillaries leads to

$$\frac{\bar{\dot{m}}_{E,\ narrow\ gasket}}{\bar{\dot{m}}_{E,\ wide\ gasket}} = \frac{r_o^2 - r_{i,w}^2}{r_o^2 - r_{i,n}^2} \tag{17}$$

For the investigated gaskets this results in a ratio of 1.31. When using the model of the branching capillaries the ratio has to be calculated as

$$\frac{\bar{\dot{m}}_{E,\ narrow\ gasket}}{\bar{\dot{m}}_{E,\ wide\ gasket}} = \frac{\ln(r_o/r_{i,w})(r_o + r_{i,w})}{\ln(r_o/r_{i,n})(r_o + r_{i,n})} \tag{18}$$

and gives a ratio of 1.46 for the investigated gaskets. For the experimental results presented in this paper an average ratio of 1.51 was found, which demonstrates, that the new model conception increases the accuracy of the prediction especially in the case of low diameter gaskets.

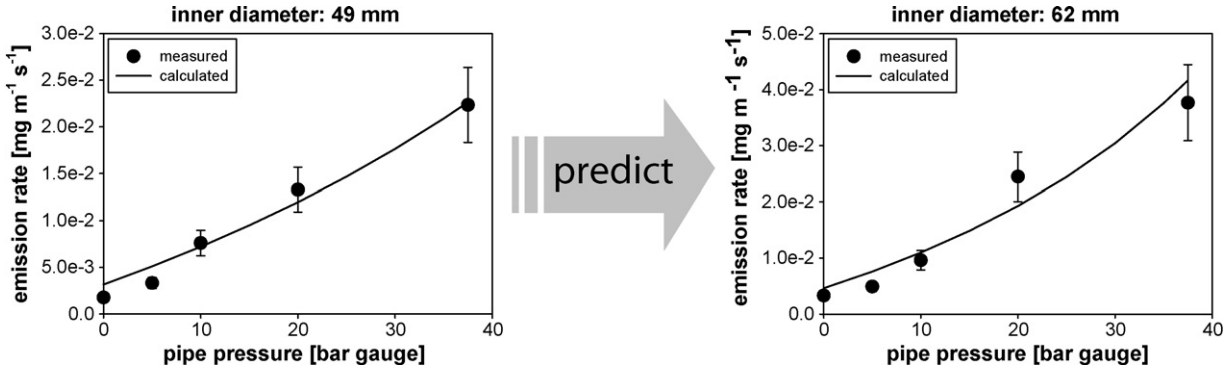

Fig. 7. Prediction of the emission rates of 1-propanol charged flange joints with Sigraflex® Universal Pro graphite sheet gaskets under variation of the gasket width and the pipe pressure (model parameters: $N_{cap} = 4.9E + 06$, $d_{cap,0} = 1.5E - 07$ m).

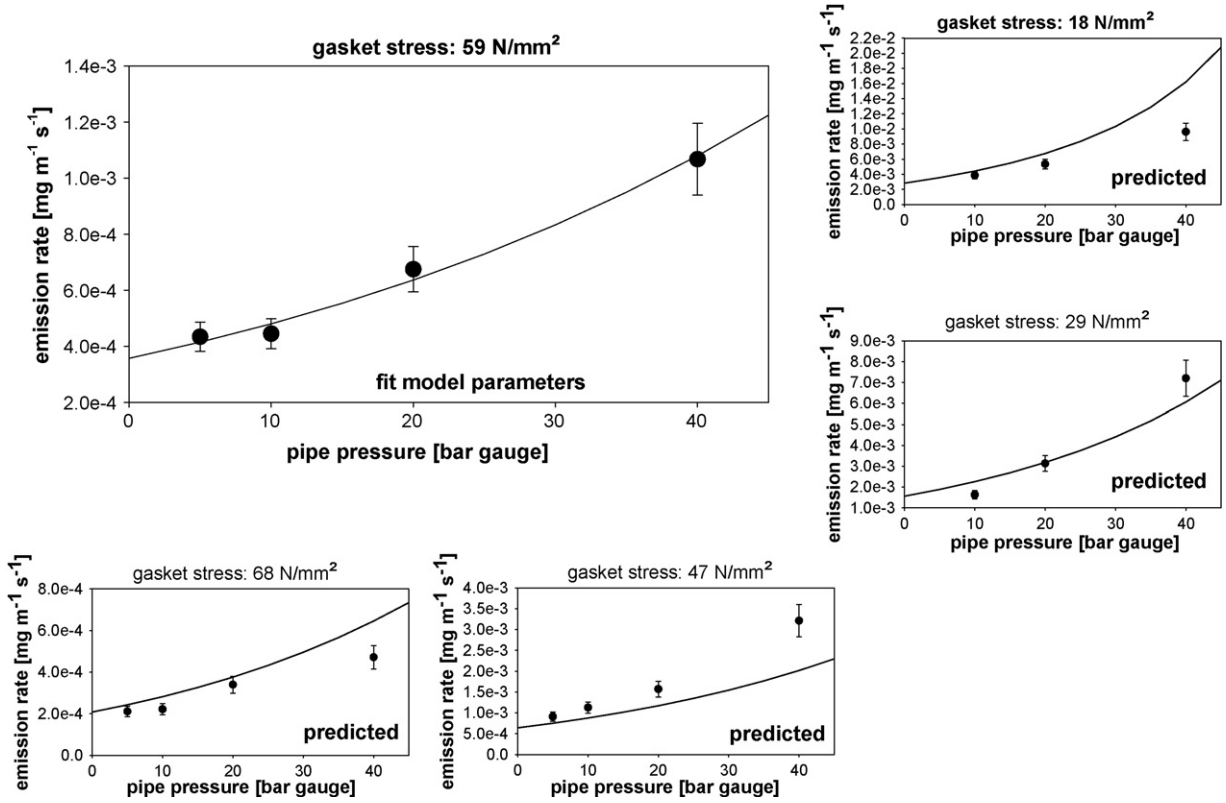

Fig. 8. Prediction of the emission rates of methanol charged flange joints with grooved gaskets for gasket stresses between 18 N/mm² and 69 N/mm² and pipe pressures between 0 bar gauge and 40 bar gauge (model parameters: $N_{cap} = 2.6E + 06$, $d_{cap,0} = 1.6E - 07$ m).

In Fig. 7 emission measurements from Fig. 1 (left side) were used to fit the model parameters capillary density N_{cap} and capillary diameter of the uncompressed gasket $d_{cap,0}$ by minimizing the sum of squared errors for a gasket with an inner diameter of 49 mm (Fig. 7, left). These parameters were used to predict the emission rates of the gasket with 62 mm inner diameter (Fig. 7, right).

The experimental results presented on the right side of Fig. 1 were used to validate the model of the influence of gasket stress on the emission rate. As the compression curve of the grooved gasket was not available, its compression behavior was approximated using the compression curve of a pure graphite sheet gasket with the same height as the two graphite layers of the grooved gasket had. Again the model parameters were determined for a gasket stress of 59 N/mm² by minimizing the sum of squared errors and the emission rates for gasket stresses of 18 N/mm², 29 N/mm², 47 N/mm² and 68 N/mm² were predicted (see Fig. 8).

Though the compression curve used for the calculations was not the original one of the investigated gasket, Fig. 8 shows, that the predicted emission rates meet the experimental results quite well.

4. Conclusions

A model describing the emission rate of VOC charged graphite gaskets was developed and validated experimentally. Analyzing the final prediction model (Eq. (16)) four parameters determining the emission rate of liquid charged flange joints could be identified: the capillary diameter of the uncompressed gasket ($d_{cap,0}$), the compression behavior of the gasket material, the gasket height (h_g) and the contact angle between the gasket material and the emitting medium, displayed by the factor $\cos(\theta)$.

The parameter with the highest impact on the emission rates of liquid charged flange joints is the capillary diameter as it occurs to the power of four in the laminar flow term and to the power of three in the capillary flow term. Guaranteeing a fine-pored gasket material therefore is a very efficient means for reducing fugitive emission rates. A possibility to improve gasket materials concerning the pore structure is to impregnate the soft material. However, this can involve a reduced tightness of the gasket at higher temperatures by pyrolytic loss of impregnation. Alternatively a very flexible gasket material can be used, so that the pore diameter will be reduced when the gasket is compressed. The mechanical stress on the gasket must therefore be as high as the total system built up by flanges, gasket and screws can bear. Here again it becomes obvious, that the assembly conditions have a major impact on fugitive emission rates of liquid charged flange joints [1], as they determine the compression of the gasket and thus the capillary diameter.

The third option for reducing fugitive emissions is minimizing the height of the gasket. However it must be taken into consideration that a gasket with little soft material has to be installed in a flange joint with very even and parallel sealing faces. Thus proper assembly becomes even more important when the gasket height is reduced [16].

In accordance with Choi et al. [12] it was found, that the application of nonwetting gasket materials that have a contact angle above 90° ($\cos(\theta) < 0$) can reduce fugitive emissions from liquid charged flange joints as they can reduce capillary driving forces.

Acknowledgements

The authors thank Mr. Notter and Mr. Skoda from Industrie- und Dichtungstechnik GmbH for providing the gaskets used in the experiments and for the support in the course of the investigations presented. We thank Mr. Zeuß from SGL Carbon Group for preparing the compression curves for the Sigraflex® Universal Pro gasket.

Furthermore very special thanks go to Jrg Hillmann, who has carried out the experiments, and to the German Federal Environmental Foundation for sponsoring this research project with a scholarship and additional financial means which made the realization of the project possible.

References

[1] C. Bramsiepe, G. Schembecker, Fugitive emissions from liquid-charged flange joints: a comparison of laboratory and field data, Environ. Sci. Technol. 43 (2009) 4498–4502.
[2] Deutsches Institut für Normung, DIN EN 13555: Flansche und ihre Verbindungen – Dichtungskennwerte und Prüfverfahren für die Anwendung der Regeln für die Auslegung von Flanschverbindungen mit runden Flanschen und Dichtungen, Deutsche Fassung EN 13555, 2005.
[3] Deutsches Institut für Normung, DIN EN 1591 Teil 1 - Flansche und ihre Verbindungen – Regeln für die Auslegung von Flanschverbindungen mit runden Flanschen und Dichtung Teil 1: Berechnungsmethode; Deutsche Fassung EN 1591-1:2001, 2001.
[4] European Sealing Association e.V. and Fluid Sealing Association, Einbauanleitung für Flachdichtungen, ISBN: 1-892965-08-9.
[5] European Sealing Association e.V. and Fluid Sealing Association, Wegweiser für eine sichere Dichtverbindung an Flanschen, ESA/FSA Publikation Nr. 009/98.
[6] Fluid Sealing Association, Sealing Sense—How Do You Select and Install the Right Gasket? Pumps & Systems 1 (2005) 22–23.
[7] Fluid Sealing Association, Sealing Sense—How Do I Determine Bolt Torque for Flanged Connections? Pumps & Systems 6 (2008) 88–90.
[8] A. Micheely, Ph.D. thesis, Universität Dortmund, 1977.
[9] W. Kämpkes, Zur Berechenbarkeit des Emissionsverhaltens von Rohrleitungs-Flanschverbindungen mit It-Flachdichtungen unter Berucksichtigung des Dichtungsmaterials und der Dichtungsgeometrie bei unterschiedlichen Betriebszuständen, Chem. Ing. Tech. 10 (1984) 790–791.
[10] C. Hummelt, D. Bathen, H. Schmidt-Traub, Emissionen an Flanschverbindungen - Verfahren zur Berechnung und Abschätzung, Chem. Ing. Tech. 11 (2001) 1408–1414.
[11] C. Hummelt, D. Bathen, Diffuse Emissionen an Flanschverbindungen: Einfluss der Flächenpressung, Chem. Ing. Tech. 5 (2000) 467–472.
[12] S.J. Choi, R.D. All, M.R. Overcash, P.K. Lim, Capillary-flow mechanism for fugitive emissions of volatile organics from valves and flanges: model development, experimental evidence, and implications, Environ. Sci. Technol. 3 (1992) 478–484.
[13] DIN 28090-2, Statische Dichtungen für Flanschverbindungen - Teil 2: Dichtungen aus Dichtungsplatten; spezielle Prüfverfahren zur Qualitätssicherung, Beuth-Verlag, Berlin, 1995.
[14] Schubert, Kapillarität in porsen Feststoffsystemen, Heidelberg, 1982.
[15] SGL Carbon Group, Data Sheet of the Sigraflex® Universal Pro gasket (thickness: 3 mm), Available via the download center of the SGL Carbon homepage: URL: http://www.sglgroup.com/.
[16] D. Bathen, Fehlerverzeihlichkeit der Dichtung an Flanschverbindungen, Dichtungstechnik 2 (2002) 59–62.
[17] S.A. Altinkaya, Predicting emission characteristics of volatile organic compounds from wet surface coatings, Chem. Eng. J. 3 (2009) 586–593.